Activating Organic Phosphorescence via Heavy Metal–π Interaction Induced Intersystem Crossing

Meng-Jia Sun, Olga Anhalt, Menyhárt B. Sárosi, Matthias Stolte, and Frank Würthner*

Heavy-atom-containing clusters, nanocrystals, and other semiconductors can sensitize the triplet states of their surface-bonded chromophores, but the energy loss, such as nonradiative deactivation, often prevents the synergistic light emission in their solid-state coassemblies. Cocrystallization allows new combinations of molecules with complementary properties for achieving functionalities not available in single components. Here, the cocrystal formation that employs platinum(II) acetylacetonate (Pt(acac)$_2$) as a triplet sensitizer and electron-deficient 1,4,5,8-naphthalene diimides (NDIs) as organic phosphors is reported. The hybrid cocrystals exhibit room-temperature phosphorescence confined in the low-lying, long-lived triplet state of NDIs with photoluminescence (PL) quantum yield (Φ_{PL}) exceeding 25% and a phosphorescence lifetime (τ_{Ph}) of 156 μs. This remarkable PL property benefits from the noncovalent electronic and spin–orbital coupling between the constituents.

1. Introduction

Unlike fluorescence, phosphorescence is emission from the lowest-energy triplet state which is normally forbidden by spin-selection rules.[1–3] For this reason, triplet states in organic semiconductors have been regarded as optically inactive or "dark" states for a long time, when phosphorescence from pure organic chromophores can only be detected under cryogenic conditions. Room-temperature phosphorescence (RTP) from organic solids has been recently sought by means of doping strategy,[4,5] i.e., doping of organic chromophores into a rigid matrix containing halogens or carbonyl groups, taking advantage of the external spin–orbital coupling (SOC) effect. While this method can moderately sensitize RTP for a number of organic emitters, only few have clearly defined single-crystal structures that reveal SOC promoting noncovalent interactions between emitter and host. Recent advances in crystal engineering show that cocrystallization can combine molecules with complementary properties and confine target molecules in a well-resolved crystalline environment, offering a new strategy to harvest "dark" triplet excitons.[6–10]

1,4,5,8-Naphthalene diimides (NDIs, for structure, see **Scheme 1**) are the smallest homolog of the rylene diimides with planar and electron-deficient aromatic core, which have been applied in fields ranging from biomedicine to organic electronics.[11–13] While the fast depopulation of the photoexcited singlet state of naphthalene diimides by intersystem crossing (ISC) has been known since a long time,[14,15] the mechanism was only clarified recently. Accordingly, recent investigations showed that after photoexcitation to the S$_1$ state (π–π*), an equilibrium between this state and the almost isoenergetic T$_n$ (n–π*) states is established before the population is funneled down to the T$_1(\pi$–π*) state via internal conversion (IC).[16,17] This progress elucidated in photophysics studies indicates that NDIs are promising organic phosphors because of their efficient triplet harvesting as well as negligible fluorescence interference.

In addition to triplet population via ISC between excited states of different multiplicity, the efficiency of phosphorescence depends on the SOC between the lowest triplet state, T$_1$, and the ground state.[18] Either covalently bonding heavy-atom functional groups to NDIs or rigidifying NDIs into heavy-atom-containing environments can enhance the SOC and sensitize its RTP.[19,20] However, these strategies often introduce unwanted competition between phosphorescence and fluorescence, in which the fluorescence originates from the charge-transfer state between the functional groups and the NDI core.[21]

Square-planar d^8 Pt(II) complexes possessing filled molecular orbitals with strong metal d character can axially interact with neighboring molecules, leading to new excited states. In addition to the Pt···Pt interaction,[22] Kukushkin and coworkers recently reported a type of π-hole···Pt(II) interaction existing in the cocrystal of perfluorinated arenes and Pt(II) complexes.[23,24] But these arenes cannot be sensitized because their large highest occupied molecular orbital–lowest unoccupied molecular orbital (HOMO–LUMO) gap prohibits
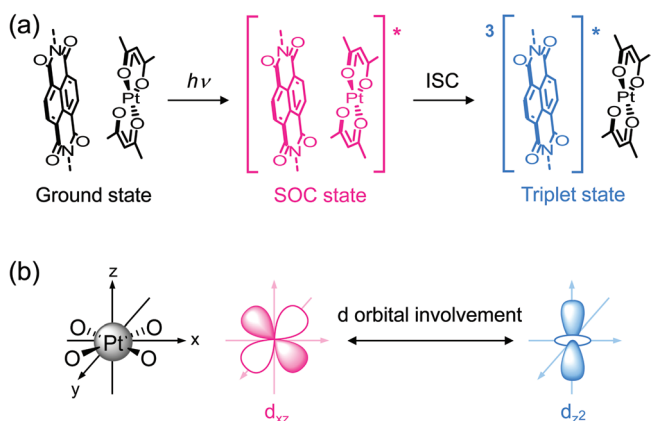
M.-J. Sun, O. Anhalt, M. B. Sárosi, M. Stolte, F. Würthner
Center for Nanosystems Chemistry (CNC)
Universität Würzburg
Theodor-Boveri-Weg, 97074 Würzburg, Germany
E-mail: wuerthner@uni-wuerzburg.de
M. Stolte, F. Würthner
Institut für Organische Chemie
Universität Würzburg
Am Hubland, 97074 Würzburg, Germany

The ORCID identification number(s) for the author(s) of this article can be found under https://doi.org/10.1002/adma.202207331.

ADVANCED
SCIENCE NEWS
www.advancedsciencenews.com

ADVANCED
MATERIALS
www.advmat.de

Scheme 1. Concept for brightening the triplet states of NDI. a) Triplet state generation in the cocrystal consisting of NDI and **Pt(acac)$_2$**. b) d orbitals centered on Pt(II) compounds which may provide significant spin–orbital coupling for the acceleration of ISC processes.

intermolecular charge-transfer (CT) transitions. Although there have been several studies on supramolecular assemblies and organometallic compounds consisting of organic chromophores and Pt(II) complexes,[25–27] to the best of our knowledge, the utilization of Pt(II) complexes to sensitize the triplet emission from the organic chromophores via noncovalent interactions has not been reported yet.

2. Results and Discussion

Here, we investigate whether RTP in NDIs could be sensitized by means of cocrystal formation with a Pt(II) complex, platinum(II) acetylacetonate (**Pt(acac)$_2$**), based on the following hypotheses: i) the similar molecular size and the electrostatic complementarity could enable them to assemble into a closely cofacial stacking motif (Figure S1, Supporting Information). ii) **Pt(acac)$_2$** acting as the triplet sensitizer, can form CT complex with NDIs via the interaction between the HOMO of **Pt(acac)$_2$** to the LUMO of NDIs (Scheme 1a and Figure S2, Supporting Information). iii) d electrons of Pt(II) are in conjugation with the π-system of the acac ligand, thus providing d-orbital contributions from d_{xz}, d_{yz}, or d_{z^2} orbitals to optical transitions with angular momentum changes, thereby promoting SOC between different spin states (Scheme 1b). This process recalls us of the metal-to-ligand charge transfer in luminescent transition metal complexes,[28,29] inspiring us to utilize it in a noncovalent way. iv) The presence of Pt(II) could provide a strong external heavy-atom effect, leading to the acceleration of the radiative rate from the locally excited lowest triplet state of NDIs.

The imide substituents of NDIs must also be taken into account for cocrystal formation, as they guide the spacing and the orientation between both components in the crystal lattice. Generally, NDIs are well-soluble if long and branched alkyl chains or bulky aryl groups are introduced at the imide position, which also diminish the molecular interactions. Here, we successfully prepared two cocrystals, **Pt-NDI1** and **Pt-NDI2**, consisting of **Pt(acac)$_2$** and two NDIs functionalized with different imide substituents, 3-pentyl (**NDI1**) and benzyl (**NDI2**),
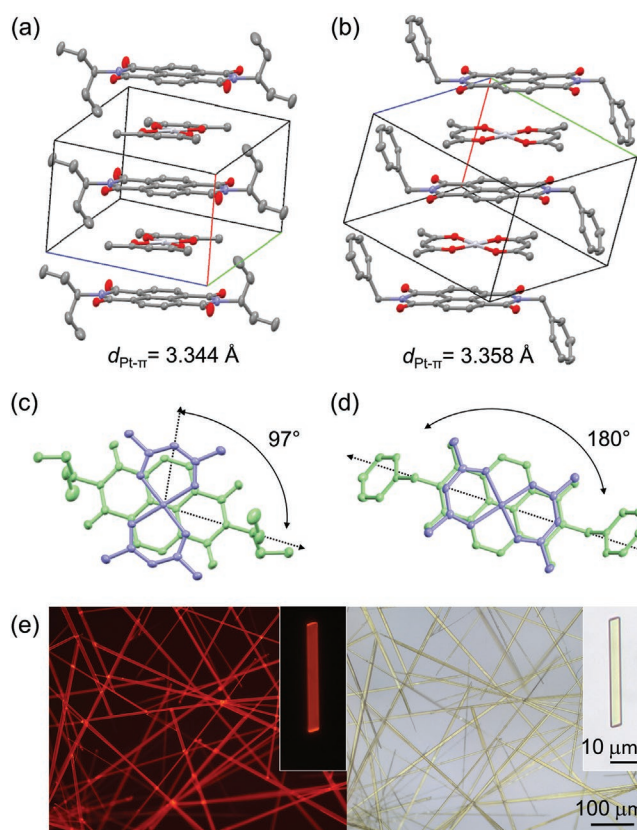

Figure 1. a,b) Packing arrangement and intermolecular distances within cocrystals of **Pt-NDI1** (a) and **Pt-NDI2** (b). c,d) H atoms and solvent molecules were omitted for clarity. Intermolecular orientation between NDI (green) and **Pt(acac)$_2$** (blue) in the stack of **Pt-NDI1** (c) and **Pt-NDI2** (d). e) Optical microscopy images of **Pt-NDI1** microcrystals under blue light excitation (left) and under bright field (right) on quartz substrates. The insets show the individual microcrystal.

through a solvent diffusion method (1:1, 0.01 M, chloroform/methanol, see the experimental details in the Supporting Information). Both light yellow cocrystals grew into long needle-like shapes and exhibit prominent red luminescence under UV irradiation (**Figure 1**e and Figures S3, Supporting Information). To further support our hypothesis, we also grow isostructural cocrystals consisting of **NDI1** and **Pd(acac)$_2$**. In contrast to **Pt-NDI1**, no phosphorescence was detected at room temperature for **Pd-NDI1**, indicating the efficient sensitization effect from the Pt center (Figures S3–S5, Supporting Information).

Single-crystal X-ray diffraction (scXRD) was conducted to identify the molecular packing within these two cocrystals. **Pt-NDI1** adopts an alternating packing between **Pt(acac)$_2$** and **NDI1** in 1:1 stoichiometry to form a 1D crystal lattice along the a-axis. The intermolecular distance ($d_{Pt-\pi}$) between the Pt(II) center to the π-surface of **NDI1** is 3.344 Å (Figure 1a and Figure S5a, Supporting Information). **Pt(acac)$_2$** stacks on top of **NDI1** in an almost orthogonal alignment with an angle of 97° between the long molecular axis of the two molecules (Figure 1c). In contrast to **Pt-NDI1**, the orientation between the long axis of **Pt(acac)$_2$** and **NDI2** is parallel (180°) at the expense of a slightly increased Pt–π distance of 3.358 Å (Figure 1b,d and Figure S5c, Supporting Information). This indicates that the

ADVANCED
SCIENCE NEWS
www.advancedsciencenews.com

ADVANCED
MATERIALS
www.advmat.de

imide groups of the NDIs play a key role in determining the orientation of **Pt(acac)₂**. In addition, we noted that one chloroform molecule cocrystallized into the unit cell of **Pt-NDI2** (Figure S5c, Supporting Information). The phase purity and stability were further confirmed by powder X-ray diffraction (pXRD). **Pt-NDI1** shows sharp diffraction peaks well-matched with the simulated data from scXRD result. However, broad, amorphous-like, and mismatched peaks were observed for **Pt-NDI2**, indicating the collapse of the cocrystal structure after being exposed to air (Figure S6, Supporting Information). Hirshfeld surface analyses[30] corroborate the presence of strong interactions between the π–π contacts of **Pt(acac)₂** and **NDI1** as well as some other close contacts between **Pt(acac)₂** and the two NDIs in the cocrystals (Figure S7, Supporting Information). The detailed cocrystal information is summarized in Table S1 in the Supporting Information.

While both cocrystals, **Pt-NDI1** and **Pt-NDI2**, are equally accessible and initially appear similar in solution, **Pt-NDI2** rapidly disassembles under ambient conditions. The release of chloroform from the crystal lattice presumably is the origin of this decomposition, which prohibits us from conducting in depth spectroscopic investigations. However, as shown in Figure 1e, **Pt-NDI1** grows into stable yellow 1D cocrystals with strong, red emission under blue light excitation (464–495 nm). The corresponding absorption spectrum of **Pt-NDI1** cocrystal, obtained from reflection measurements in BaSO₄ trituration, exhibits not only absorption characteristic of its two monomer components **Pt(acac)₂** and **NDI1** but also a new, broad absorption band between 430 and 550 nm (**Figure 2**a and Figure S8, Supporting Information). This new transition is attributed to an intermolecular charge transfer (CT) from the d-orbital involving HOMO of **Pt(acac)₂** to the LUMO of **NDI1** (Figure S2a, Supporting Information).[28] The orientation of this CT is also estimated by polarization microscopy study, in which the individual cocrystal becomes slightly brighter (darker) under green excitation (bright field) when the excitation polarization is along with the long axis of individual cocrystal (Figures S9 and S10, Supporting Information).

Pt-NDI1 crystalline powder exhibits solid-state PL at ambient condition with a long-lived, monoexponential decay (156 μs) and a high Φ_{PL} of 25.1 ± 1% (λ_{ex} = 480 nm, Figure 2a and Figure S11, Supporting Information). The PL spectrum features distinct vibronic progressions at 625, 688, and 763 nm, which matches well with that of individual microcrystals and closely resembles the phosphorescence spectrum of free **NDI1** sensitized by ethyl iodide in frozen chloroform at 77 K (Figure S12a,b, Supporting Information). The phosphorescence lifetime of **NDI1** sensitized by ethyl iodide (3 ms) is much shorter than that without sensitization (38 ms, Figure S12c,d, Supporting Information), indicating the external heavy atom effect provided by iodide strongly increases the radiative rate from the spin-forbidden triplet state to the ground state. This effect is in line with the phosphorescent character of **Pt-NDI1**, in which the Pt heavy atom enhances ISC in its complex with closely stacked organic molecules as observed for other heavy-metal-containing adducts involving Hg and Ag atoms.[31] **Pt-NDI2** shows slightly red-shifted PL spectra (650, 715, 795 nm) compared to **Pt-NDI1**, but degrades rapidly due to its structural instability (Figure S13, Supporting Information), which prohibited further characterization.

The phosphorescence of **Pt-NDI1** is further elucidated by excitation-wavelength (λ_{ex})-dependent PL mapping and time-resolved emission spectra (TRES) at room temperature. PL mapping shows that the shape of the spectrum is independent of λ_{ex}, varying from 250 to 550 nm (Figure 2b). Additionally, the Φ_{PL} of **Pt-NDI1** does not depend on λ_{ex} (Figure S11, Supporting Information). TRES reveals that no other new emission bands can be observed at various delay times (Figure S14, Supporting Information) These indicate that the PL of **Pt-NDI1** obeys Kasha's rule where emission takes place from the lowest excited state, here T_1 of **NDI1**.[18]

To gain deeper insights into the photophysical process, we investigated the excited-state characteristics of **Pt-NDI1** complex by time-dependent density functional theory calculations on a model system of the respective cocrystal. In **Pt-NDI1(H)**
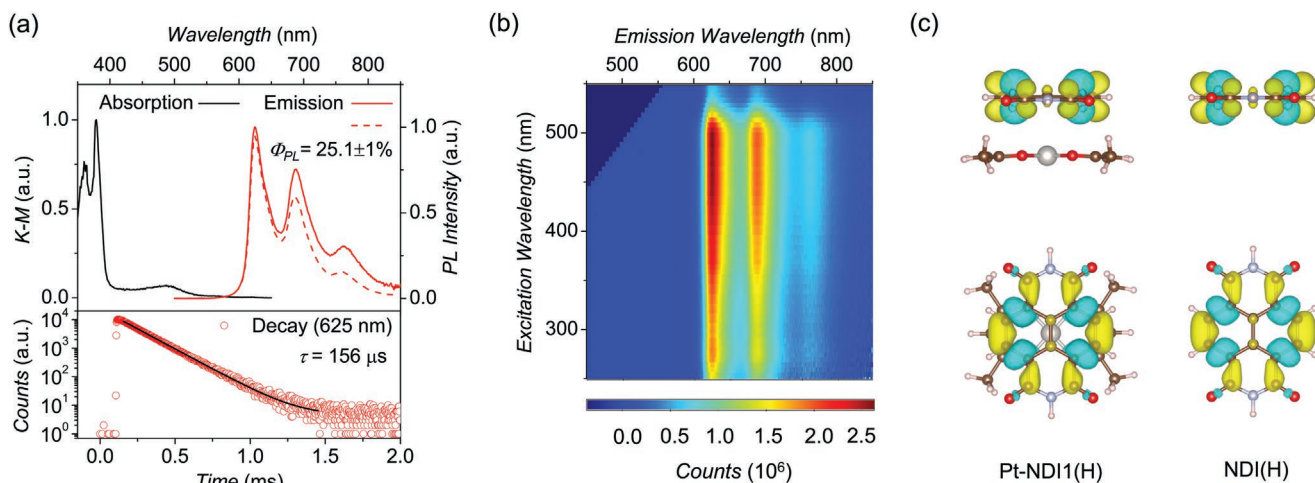

Figure 2. a) UV–vis absorption (black solid line), photoluminescence (λ_{ex} = 480 nm, red line), and decay (λ_{ex} = 480 nm, red circles) of **Pt-NDI1** cocrystals at room temperature. The PL of an individual microcrystal is displayed as red dotted line. b) Excitation-dependent photoluminescence mapping of **Pt-NDI1** cocrystal at room temperature. c) Difference densities of T_1 in **Pt-NDI1(H)** complex (left) and in pure **NDI(H)** (right), (top, front view; bottom, top view). The loss of electron density with respect to the S_0 state is indicated in cyan and the gain in yellow. Isovalue: 0.001 [e Å⁻³]½.

complex, where the imide substituents are replaced by hydrogen atoms (Figure S1b, Supporting Information), the electronic structures are no longer pure singlets or triplets, but are strongly mixed states, SOC states, which are composed of certain singlet and triplet transitions with large SOC matrix elements (SOCMEs) (Figure S15, Supporting Information). The large SOCMEs originate from several transitions between low-lying S_n singlet and T_n triplet states with different d-orbital character at the Pt(II) center, enabling a change in the spin angular momentum. In contrast, the lowest energy SOC state is in fact the pure T_1 state exhibiting a local excitation (LE) character, in which the electron and hole distributions are mostly confined in the NDI counterpart (Figure 2c). Thus, for those transitions the presence of heavy atoms enables ultrafast ISC from the higher-level singlet states to the triplet manifold that can compete with IC to the S_1 state.[16] These results are in accordance with spin selection rules, in which different d orbitals coupled by the angular momentum at the same center lead to significant SOC.[29] Therefore, we propose that the triplet exciton is first populated to SOC states with hybrid features of singlets and triplets via either ISC from SOC states with singlet character or direct excitation to SOC states with T_n ($n > 1$) character, and then is funneled down to T_1 through IC. Thus, via experimental photophysical investigations combined with theoretical calculations, we propose that the RTP of **Pt-NDI1** originates from the T_1 state confined in **NDI1**. The origin of SOC in **Pt-NDI2** is quite similar to that of **Pt-NDI1**, in which different d orbital-involving transitions play key roles (Figure S16, Supporting Information). The T_1 state of **Pt-NDI2** has a lower energy and a larger CT transition component from **Pt(acac)₂** to **NDI2(H)**, which may explain the slightly red-shifted emission, in comparison to **Pt-NDI1**. In contrast to Pt-containing systems, there is no or negligible mixing of singlet and triplet states in **Pd-NDI1(H)**, probably because the reduced atomic mass of Pd is inadequate to introduce strong enough SOC (Figure S17, Supporting Information).

Complementary information on the phosphorescence process is obtained from a temperature (*T*)-dependent PL study which proved to be fully reversible. **Figure 3**a shows the PL evolution of **Pt-NDI1** upon cooling from 298 down to 80 K. The PL intensity increases with a slight blue shift from 298 to 140 K along with an increase of lifetime, due to the suppression of thermal vibrations. The increase of lifetime in this range is moderate because the cocrystal acts as a solid matrix that isolates and rigidifies **NDI1**, which reduces the nonradiative decay to a large extent. Afterward the PL intensity starts to decrease from 140 to 80 K, accompanied by a reduction of lifetime from 181 to 168 μs (Figure S18 and Table S2, Supporting Information). The *T*-dependent evolutions between PL intensity and lifetime match well, and the PL exhibits a thermally activated behavior at low *T* (Figure 3b). In general, PL intensity and lifetime both increase with decreasing *T* due to the suppression of nonradiative energy loss. The phenomenon observed from 80 to 140 K is accordingly quite unusual and might originate from several competing pathways to the radiative deactivation. One possible explanation may be that SOC between T_1 and the ground state reduces with increasing *T* due to vibronic effects, which results in an increase in lifetime. The increase in PL intensity could be due to a thermally activated ISC from an SOC state with singlet character to T_n.

3. Conclusion

The phosphorescence of NDIs is successfully sensitized by a triplet sensitizer, **Pt(acac)₂**, at room temperature, by means of cocrystal formation. Different d-orbital transitions between singlet and triplet states enable significant SOC, activating the spin-flip process. The external heavy-atom effect caused by the Pt(II) makes the spin-forbidden transition from the T_1 to the ground state more allowed, promoting the triplet radiative decay. **Pt-NDI1** emits strong phosphorescence at room temperature from its low-lying, long-lived triplet state confined in **NDI1** with a remarkable high Φ_{PL} exceeding 25% and a phosphorescence lifetime, τ_{Ph}, of 156 μs. To our best knowledge, this is the highest reported Φ_{PL} for NDI phosphors (Figure S19a, Supporting Information). Together with the 20 times faster radiative decay of **Pt-NDI1** (1.67×10^3 s^{-1}) compared to reported
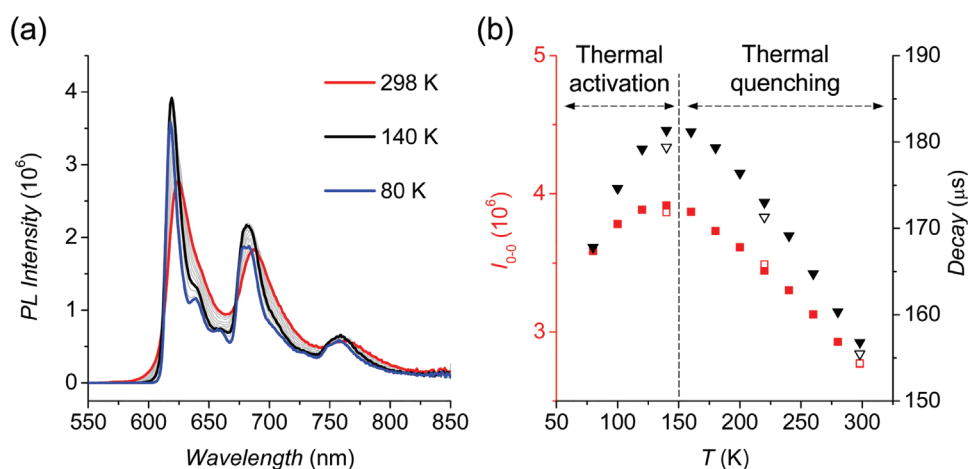

Figure 3. Temperature (*T*)-dependent PL study of **Pt-NDI1** ($\lambda_{ex} = 480$ nm). a) Evolution of PL spectrum of **Pt-NDI1** from 298 (red) to 80 K (blue). b) Plot of the *T*-dependent PL maxima intensity (red solid squares) and lifetime decay (black solid triangles) of **Pt-NDI1**. The backward scan of PL intensity and lifetime decay were shown as open squares and triangles, respectively.

halogen-containing phosphorescent co-crystals (Figure S19b, Supporting Information), we may envision the application of such complexes in display technologies. We anticipate this cocrystallization strategy will be generalizable and broadly applicable to sensitize the phosphorescence between square-planar Pt(II) complexes and organic π-scaffolds via host–guest complexation and crystal engineering.

Supporting Information

Supporting Information is available from the Wiley Online Library or from the author.

Conflict of Interest

The authors declare no conflict of interest.

Data Availability Statement

The data that support the findings of this study are available from the corresponding author upon reasonable request.

[1] S. Hirata, *Appl. Phys. Rev.* **2022**, *9*, 011304.
[2] D. Sasikumar, A. T. John, J. Sunny, M. Hariharan, *Chem. Soc. Rev.* **2020**, *49*, 6122.
[3] A. Köhler, H. Bässler, *Mater. Sci. Eng., R* **2009**, *66*, 71.
[4] a) S. Kuila, S. J. George, *Angew. Chem., Int. Ed.* **2020**, *59*, 9393; b) S. Hirata, K. Totani, J. Zhang, T. Yamashita, H. Kaji, S. R. Marder, T. Watanabe, C. Adachi, *Adv. Funct. Mater.* **2013**, *23*, 3386.
[5] W. Qiu, X. Cai, M. Li, Z. Chen, L. Wang, W. Xie, K. Liu, M. Liu, S.-J. Su, *J. Phys. Chem. Lett.* **2021**, *12*, 4600.
[6] L. Sun, W. Zhu, X. Zhang, L. Li, H. Dong, W. Hu, *J. Am. Chem. Soc.* **2021**, *143*, 19243.
[7] L. Sun, Y. Wang, F. Yang, X. Zhang, W. Hu, *Adv. Mater.* **2019**, *31*, 1902328.
[8] W. Zhu, L. Zhu, Y. Zou, Y. Wu, Y. Zhen, H. Dong, H. Fu, Z. Wei, Q. Shi, W. Hu, *Adv. Mater.* **2016**, *28*, 5954.
[9] M.-J. Sun, Y. Liu, W. Zeng, Y. S. Zhao, Y.-W. Zhong, J. Yao, *J. Am. Chem. Soc.* **2019**, *141*, 6157.
[10] S. K. Park, J. H. Kim, T. Ohto, R. Yamada, A. O. F. Jones, D. R. Whang, I. Cho, S. Oh, S. H. Hong, J. E. Kwon, J. H. Kim, Y. Olivier, R. Fischer, R. Resel, J. Gierschner, H. Tada, S. Y. Park, *Adv. Mater.* **2017**, *29*, 1701346.
[11] S.-L. Suraru, F. Würthner, *Angew. Chem., Int. Ed.* **2014**, *53*, 7428.
[12] N. Sakai, J. Mareda, E. Vauthey, S. Matile, *Chem. Commun.* **2010**, *46*, 4225.
[13] M. Al Kobaisi, S. V. Bhosale, K. Latham, A. M. Raynor, S. V. Bhosale, *Chem. Rev.* **2016**, *116*, 11685.
[14] G. P. Wiederrecht, W. A. Svec, M. R. Wasielewski, T. Galili, H. Levanon, *J. Am. Chem. Soc.* **1999**, *121*, 7726.
[15] P. Ganesan, J. Baggerman, H. Zhang, E. J. R. Sudhölter, H. Zuilhof, *J. Phys. Chem. A* **2007**, *111*, 6151.
[16] O. Yushchenko, G. Licari, S. Mosquera-Vazquez, N. Sakai, S. Matile, E. Vauthey, *J. Phys. Chem. Lett.* **2015**, *6*, 2096.
[17] A. Aster, C. Rumble, A.-B. Bornhof, H.-H. Huang, N. Sakai, T. Šolomek, S. Matile, E. Vauthey, *Chem. Sci.* **2021**, *12*, 4908.
[18] N. J. Turro, V. Ramamurthy, J. C. Scaiano, *Modern Molecular Photochemistry of Organic Molecules*, University Science Books, Sausalito, CA, USA **2010**.
[19] S. Kuila, K. V. Rao, S. Garain, P. K. Samanta, S. Das, S. K. Pati, M. Eswaramoorthy, S. J. George, *Angew. Chem., Int. Ed.* **2018**, *57*, 17115.
[20] Y. Liu, W. Wu, J. Zhao, X. Zhang, H. Guo, *Dalton Trans.* **2011**, *40*, 9085.
[21] S. Kuila, S. Garain, S. Bandi, S. J. George, *Adv. Funct. Mater.* **2020**, *30*, 2003693.
[22] V. W.-W. Yam, K. M.-C. Wong, N. Zhu, *J. Am. Chem. Soc.* **2002**, *124*, 6506.
[23] A. V. Rozhkov, I. V. Ananyev, R. M. Gomila, A. Frontera, V. Y. Kukushkin, *Inorg. Chem.* **2020**, *59*, 9308.
[24] A. V. Rozhkov, M. A. Krykova, D. M. Ivanov, A. S. Novikov, A. A. Sinelshchikova, M. V. Volostnykh, M. A. Konovalov, M. S. Grigoriev, Y. G. Gorbunova, V. Y. Kukushkin, *Angew. Chem., Int. Ed.* **2019**, *58*, 4164.
[25] M. Yoshizawa, K. Ono, K. Kumazawa, T. Kato, M. Fujita, *J. Am. Chem. Soc.* **2005**, *127*, 10800.
[26] Y. Tanaka, K. M.-C. Wong, V. W.-W. Yam, *Chem. - Eur. J.* **2013**, *19*, 390.
[27] M. Schulze, A. Steffen, F. Würthner, *Angew. Chem., Int. Ed.* **2015**, *54*, 1570.
[28] S. Di Bella, I. Fragala, G. Granozzi, *Inorg. Chem.* **1986**, *25*, 3997.
[29] A. F. Rausch, H. H. H. Homeier, H. Yersin, in *Photophysics of Organometallics* (Ed: A. J. Lees), Springer, Berlin/Heidelberg, Germany, **2010**, pp. 193–235.
[30] M. A. Spackman, D. Jayatilaka, *CrystEngComm* **2009**, *11*, 19.
[31] a) M. A. Omary, R. M. Kassab, M. R. Haneline, O. Elbjeirami, F. P. Gabbaï, *Inorg. Chem.* **2003**, *42*, 2176; b) S.-Z. Zhan, F. Ding, X.-W. Liu, G.-H. Zhang, J. Zheng, D. Li, *Inorg. Chem.* **2019**, *58*, 12516.